6-2008

Transmembrane domain length of viral K+ channels is a signal for mitochondria targeting

Jorg Balss
Technische Universität Darmstadt

Panagiotis Papatheodorou
Ruhr-Universitat Bochum

Mario Mehmel
Technische Universität Darmstadt

Dirk Baumeister
Technische Universität Darmstadt

Brigitte Hertel
Technische Universität Darmstadt

See next page for additional authors

Transmembrane domain length of viral K^+ channels is a signal for mitochondria targeting

Jörg Balss*, Panagiotis Papatheodorou†, Mario Mehmel*, Dirk Baumeister*, Brigitte Hertel*, Nicolas Delaroque‡, Franck C. Chatelain§, Daniel L. Minor, Jr.§, James L. Van Etten¶‖, Joachim Rassow†, Anna Moroni**, and Gerhard Thiel*‖

*Institute of Botany, Technische Universität Darmstadt, D-64287 Darmstadt, Germany; †Institute for Physiological Chemistry, Ruhr-Universität Bochum, D-44780 Bochum, Germany; ‡Max Planck Institute of Chemical Ecology, D-07745 Jena, Germany; §Cardiovascular Research Institute, University of California, San Francisco, CA 94158-2330; ¶Department of Plant Pathology and Nebraska Center for Virology, University of Nebraska, Lincoln, NE 68583-0722; and **Department of Biology and Consiglio Nazionale delle Ricerche, Istituto di Biofisica-Mi, Università degli Studi, 20133 Milano, Italy

Contributed by James L. Van Etten, June 13, 2008 (sent for review January 2, 2008)

K^+ channels operate in the plasma membrane and in membranes of organelles including mitochondria. The mechanisms and topogenic information for their differential synthesis and targeting is unknown. This article describes 2 similar viral K^+ channels that are differentially sorted; one protein (Kesv) is imported by the Tom complex into the mitochondria, the other (Kcv) to the plasma membrane. By creating chimeras we discovered that mitochondrial sorting of Kesv depends on a hierarchical combination of N- and C-terminal signals. Crucial is the length of the second transmembrane domain; extending its C terminus by ≥2 hydrophobic amino acids redirects Kesv from the mitochondrial to the plasma membrane. Activity of Kesv in the plasma membrane is detected electrically or by yeast rescue assays only after this shift in sorting. Hence only minor structural alterations in a transmembrane domain are sufficient to switch sorting of a K^+ channel between the plasma membrane and mitochondria.

algal viruses | dual targeting | K+ channel sorting | PBCV-1 | Esv-1

Viruses often serve as tools to solve basic questions in biochemistry and structure biology. For example, many biochemical pathways have been discovered because viruses commandeer the cellular machinery for transcription, translation, and protein targeting and use these pathways for their own purposes. Thus, analyses of these viral pathways have helped to uncover many basic cellular mechanisms, which otherwise would have been difficult to study (1). Likewise, because of their small size, structural studies on virus proteins have often served to understand the basic architectural features of more complex homologous proteins (2).

A current topic in cell biology that can be studied with viral proteins is the question of how structurally similar membrane proteins or even the same protein are targeted to either the endoplasmic reticulum (ER) or the mitochondria (3, 4). Hydrophobic membrane proteins such as ion channels, which end up in the plasma membrane, are generally cotranslationally targeted into the ER and then shuttled through the secretory pathway to their final destination. Targeting nascent polypeptide chains to the ER is mediated by a hydrophobic signal sequence, which eventually guides the protein to the translocon (5). However, the same type or very similar proteins, which are functional in the plasma membrane, are also located in other membrane-enclosed compartments, such as mitochondria or chloroplasts (3, 4, 6). One example of such dual localization is K^+ channels; for example the Kv1.3 channel is present in both the plasma membrane and in the inner membrane of the mitochondria (7). At present it is not understood how these proteins are targeted to the mitochondria. One possibility is that they are synthesized in the cytoplasm and sorted directly to the mitochondria. The mechanisms and topogenic information in the proteins, which are responsible for the differential synthesis and targeting of similar membrane proteins, are unknown.

We have recently identified a protein (Kcv) encoded by *Paramecium bursaria* chlorella virus (PBCV-1) (family *Phycodnaviridae*) that forms a functional K^+ channel in heterologous cells (8). Kcv has a monomer size of 94 aa and is the smallest protein known to form a functional K^+ channel. Nonetheless, Kcv is predicted to have all of the structural features typical of eukaryotic and prokaryotic K^+ channels (8, 9). Heterologous expression of Kcv, as well as reconstitution in planar lipid bilayers, results in a characteristic K^+-selective, Ba^{2+}-sensitive, and moderately voltage-dependent conductance (8–10). This means that this small viral protein contains all of the information for targeting the protein to the plasma membrane. The present study compares Kcv with another viral K^+ channel, Kesv. The Kesv channel is coded by virus EsV-1 (*Ectocarpus siliculosus* virus-1); like PBCV-1, EsV-1 is a member of the family *Phycodnaviridae*. The Kesv protein is 124 aa long, and it is predicted to form a 2-transmembrane domain (TMD) K^+ channel that is structurally similar to Kcv and to eukaryotic K^+ channels (11). Data presented in this report show that, despite their structural similarity, the 2 viral K^+ channels are sorted to different cellular compartments. Kcv enters the secretory pathway and reaches the plasma membrane, where it produces a measurable conductance. The second channel, Kesv, is sorted to the mitochondria. Mutational analyses and domain exchange experiments between the 2 channels resulted in the identification of 2 sorting signals in Kesv: a mitochondrial targeting sequence located at the N terminus, and structural features in the downstream end of the second TMD. Modifications of the latter allow switching of channel sorting between mitochondria and the secretory pathway. These results suggest that a competition between sorting signals determines the destination of a K^+ channel protein.

Results

K^+ Channel Gene in EsV-1. The genome of the phycodnavirus EsV-1 contains a 124-codon ORF (ORF 223) with all of the elements (e.g., 2 TMDs, selectivity filter) of a eukaryotic K^+ channel [11; supporting information (SI) Fig. S1*A*]. Overall, the protein, named Kesv (12), has 29% amino acids identity with the prototype K^+ channel protein Kcv from virus PBCV-1; however, the C-terminal portion of the 2 proteins has 41% amino acids

Author contributions: J.B., D.L.M., J.L.V.E., J.R., and G.T. designed research; J.B., P.P., M.M., D.B., B.H., F.C.C., and A.M. performed research; N.D. contributed new reagents/analytic tools; J.L.V.E., J.R., A.M., and G.T. analyzed data; and J.L.V.E., A.M., and G.T. wrote the paper.

The authors declare no conflict of interest.

Freely available online through the PNAS open access option.

‖To whom correspondence may be addressed. E-mail: jvanetten@unlnotes.unl.edu or thiel@bio.tu-darmstadt.de.

This article contains supporting information online at www.pnas.org/cgi/content/full/0805709105/DCSupplemental.

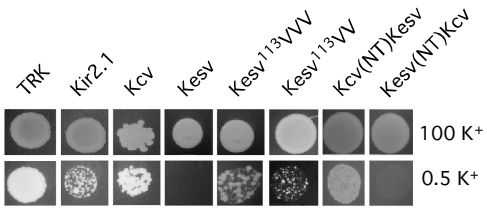

Fig. 1. Growth phenotype of yeast Δ*trk*Δ*trk2* mutants transformed with different K^+ channels or a K^+ transporter. Yeast cells were transformed with genes encoding either homologous TRK1, human Kir2.1 channel, or the viral channels Kcv or Kesv, as well as with mutants in which the second TMD of Kesv was extended at position 113 by 3 ($Kesv^{113}VVV$) or 2 valines ($Kesv^{113}VV$). In addition, yeast cells were transformed with a chimera in which the N terminus of Kcv was replaced with the N terminus of Kesv (Kcv(NT)Kesv), or vice versa (Kesv(NT)Kcv). All yeasts were grown on medium containing either 100 mM or 0.5 mM K^+. Only yeast transformed with Kesv and Kesv(NT)Kcv failed to grow on low-K^+ medium.

identity (Fig. S1*A*). Accordingly, the 2 proteins have similar hydrophobicity profiles (Fig. S1*B*).

To examine Kesv function we used yeast rescue experiments to test whether Kesv could function as a plasma membrane K^+ channel. Double mutants of yeast (Δtrk1, Δtrk2) are deprived of their endogenous K^+ uptake systems and fail to grow in low-K^+ medium (13); they only survive in a medium with high K^+ concentrations (Fig. 1, *Top* row). When these mutants are transformed with the homologous TRK1, the human Kir2.1, or the viral Kcv genes, they regain the ability to grow in medium with low (0.5 mM) K^+ concentrations (Fig. 1). However, when the yeast mutants are transformed with Kesv, the cells are unable to grow in low-K^+ medium (Fig. 1).

The results of these experiments suggest that Kcv forms an active plasma membrane K^+ channel, whereas Kesv does not. This assumption is consistent with electrophysiologic results: when Kesv or a Kesv-GFP chimera (Kesv:GFP) were expressed in either HEK293 cells or *Xenopus* oocytes we observed, in contrast to the results from a previous study (12), only an occasional up-regulation of endogenous currents but no appreciable K^+ conductance (Fig. S2).

Kesv Is Sorted to the Mitochondria. Figs. 2*A* and *B* show the cellular distribution of Kcv:GFP and Kesv:GFP in HEK293 cells, respectively. Kcv:GFP has a tubular-like distribution, indicating that it is located in membranes (Fig. 2*A*). A prominent ring-like staining always occurs around the nucleus owing to staining of the ER. The location of Kcv in the secretory pathway and in the plasma membrane is consistent with the ability to record a Kcv-mediated conductance in transfected HEK293 cells (10) and to rescue K^+ transport–deficient yeast mutants (Fig. 1).

To test the bioinformatic prediction that Kesv is targeted to the mitochondria (Table S1) HEK293 cells were incubated with MitoTracker red (Invitrogen). Fig. 2*Aa–c* and 2*Ba–c* show typical images of HEK293 cells transfected with either Kcv:GFP or Kesv:GFP, respectively, and stained with the fluorescent mitochondrial marker. The red channel shows that the MitoTracker stains internal structures with the typical hallmarks of mitochondria. An overlay of the images with MitoTracker red and GFP shows a pronounced colocalization of the colors, indicating that Kesv:GFP is located in the mitochondria (Fig. 2*Bc* and *d*, colocalization coefficient: 0.36 ± 0.09 [$n = 16$]). A similar analysis of Kcv:GFP-expressing HEK293 cells shows that GFP and MitoTracker fluorescence are different (Fig. 2*Ac* and *d*). The occasional colocalization at the edges of the mitochondria is due to limited resolution of the mitochondria from adjacent GFP-containing structures (Fig. 2*Ac*, *Inset*). The mean

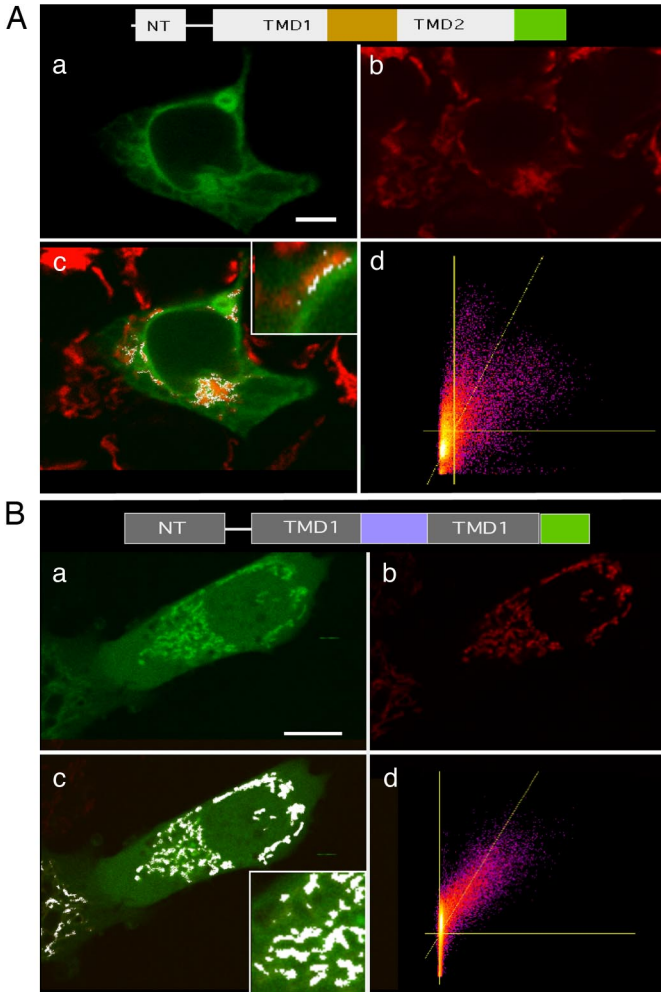

Fig. 2. Differential colocalization of Kcv:GFP and Kesv:GFP with MitoTracker in HEK293 cells. (*A*) *(Upper)* Color-coded structural elements of Kcv:GFP chimera comprising TM1 and TM2, N-terminal domain (NT) (all in light gray), pore (orange), and GFP (green). Confocal image of exemplary HEK293 cell expressing Kcv:GFP (*Aa*) and staining of the same cell with MitoTracker red (*Ab*). Overlay of the 2 images in which colocalization of the 2 colors is shown in white (*Ac*). *Inset* magnifies a region of the cell and shows that the green and red fluorescence are well separated. The apparent colocalization only results from an insufficient resolution of the red-stained mitochondria and the green-stained perinuclear ring. (*Ad*) Scatter plot of green and red pixels from region of interest (borders of green fluorescing cell). The yellow bars show thresholds for both colors. The dashed line provides linear regression solution. Pearson's colocalization coefficient in the present example is 0.12. (*B*) *(Upper)* Color-coded structural elements of Kesv:GFP chimera comprising TM1 and TM2, N-terminal domain (NT) (all in dark gray), pore (blue), and GFP (green). Confocal image of exemplary HEK293 cell expressing Kesv:GFP (*Ba*) and staining of the same cell with MitoTracker red (*Bb*). Overlay of the 2 images in which colocalization of the 2 colors is shown in white (*Bc*). *Inset* magnifies a region of the cell and shows that the green and red fluorescence colocalize. (*Bd*) Scatter plot of green and red pixels as in Fig. 2*A*. Pearson's colocalization coefficient in this example is 0.36.

colocalization coefficient in Kcv:GFP-expressing cells is 0.14 ± 0.08 ($n = 16$) and significantly ($P < 0.0001$) lower than that obtained for Kesv:GFP-expressing cells [0.36 ± 0.09 ($n = 16$)].

Kesv:GFP differs as predicted from Kcv:GFP; it is not targeted to the secretory pathway but to the mitochondria. However, the images also reveal a high GFP background in the cytoplasm. The reason for this is not known, but the results indicate that any signal recognition machinery involved in mitochondrial sorting is probably not perfect.

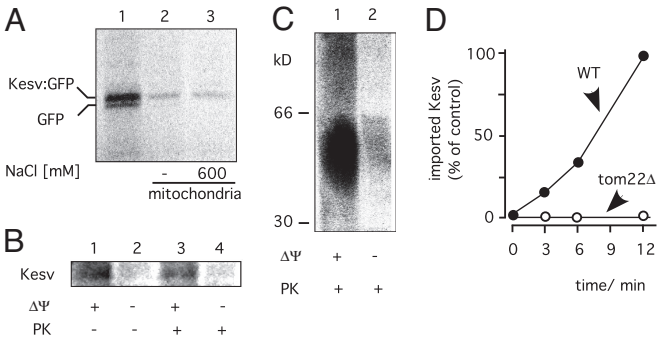

Fig. 3. Import of Kesv into isolated mitochondria *in vitro*. (*A*) Kesv:GFP and GFP were synthesized in the presence of [^{35}S]methionine in reticulocyte lysate and incubated with isolated yeast mitochondria for 10 min at 25°C. The mitochondria were subsequently re-isolated by centrifugation, resuspended in the absence (lane 2) or presence of 600 mM NaCl (lane 3), and again re-isolated. The proteins were separated by SDS/PAGE and analyzed using a PhosphorImager. An aliquot of the reticulocyte lysate was included as a standard (lane 1). (*B*) ^{35}S-labeled Kesv was synthesized in reticulocyte lysate and incubated with isolated yeast mitochondria for 10 min. As indicated, the samples contained valinomycin (-ΔΨ), or the mitochondria were subsequently treated with proteinase K (+ PK). The mitochondria were re-isolated and analyzed by SDS/PAGE. (*C*) Radiolabeled Kesv was imported into mitochondria as in *B*, and the mitochondria were re-isolated and lysed in the presence of digitonin. The proteins were separated by blue native PAGE. (*D*) Kesv was imported into mitochondria that were in parallel isolated from a *tom22*Δ strain (14) or from the corresponding WT strain. Samples were removed after different times of incubation as indicated and treated with proteinase K. The proteins were separated by SDS/PAGE, and the relative amounts were determined using a PhosphorImager. The highest value was set to 100% (control).

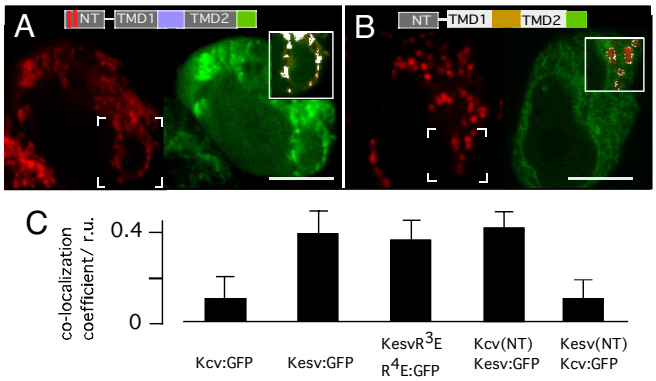

Fig. 4. The N terminus does not determine targeting of viral K^+ channels. *Upper* in *A* and *B*: color-coded structural elements of chimeras (see Fig. 2). The location of mutations is indicated by red bars. (*A* and *B*) Images of GFP (green) and MitoTracker (red) channels from confocal images of exemplary HEK293 cells expressing different chimeras of Kesv:GFP or Kcv:GFP. *Insets* show overlay of the green and red channels from areas indicated. White pixels highlight areas of maximal colocalization. (*A*) Kesv:GFP channel with mutations (R^3E, R^4E) in the N terminus. (*B*) Chimera of N terminus of Kesv plus Kcv (Kesv(NT)Kcv:GFP). (*C*) Pearson's colocalization coefficient (*P*) for GFP and MitoTracker red in HEK293 cells expressing the constructs listed.

Kesv Is Actively Imported into Mitochondria. To examine the mitochondrial localization of Kesv further, the Kesv:GFP chimera and GFP alone (as a control) were translated *in vitro* and incubated with isolated mitochondria from yeast. The ^{35}S-labeled Kesv:GFP and GFP proteins are detected separately (Fig. 3*A*, lane 1). After re-isolation of the mitochondria only Kesv:GFP remained associated with the mitochondria (Fig. 3*A*, lane 2). Further incubation of the isolated mitochondria with 600 mM NaCl did not disrupt the association of the protein with the mitochondria (Fig. 3*A*, lane 3), indicating a tight association.

To test whether Kesv is imported into mitochondria, *in vitro*–translated and ^{35}S-labeled Kesv protein was incubated with isolated yeast mitochondria in the presence and absence of a membrane potential. The data in Fig. 3*B* show that Kesv is only imported in the presence of a membrane potential and that after uptake into mitochondria, Kesv is protected against externally added proteinase K. The results of these experiments suggest that the K^+ channel is imported into the mitochondria in a voltage-dependent manner.

To examine the oligomeric state of the imported channel the ^{35}S-labeled Kesv protein was imported into isolated mitochondria as reported above. After removal of externally associated protein by incubation with proteinase K and re-isolation, the mitochondria were lysed by digitonin and the mitochondrial proteins separated by blue native PAGE (Fig. 3*C*). A specific macromolecular complex of ≈40 kDa was detected only under conditions that favored uptake of Kesv. The molecular weight of this complex is similar to that predicted for a Kesv tetramer. The results of these experiments suggest that the K^+ channel is present in the mitochondria as a functional tetramer.

To examine the import pathway of Kesv into the mitochondria we performed the same kind of import experiments with isolated mitochondria from either WT yeast or from yeast mutants without Tom22 (*tom22*Δ) (14). The Tom22 protein is an important component of the canonical mitochondrial import machinery; the absence of this protein destabilizes the TOM complex (Fig. S3) and greatly reduces protein uptake by this pathway (14). A quantification of the import of radiolabeled Kesv into the mitochondria shows that the mitochondria from the mutant yeast fail to accumulate Kesv (Fig. 3*D*). The results of these experiments indicate that Kesv is actively imported into mitochondria and that the outer membrane TOM complex is involved in the uptake of the protein.

The N Terminus of Kesv Is Not Essential for Mitochondrial Sorting. Kesv has a hydrophobic N-terminal domain, which is longer than its Kcv counterpart (12; Fig. S1). This N terminus reveals several positive amino acids that, together with the predicted α-helical structure, are typical properties of a signal peptide for mitochondrial targeting (15). Predictions indicated that Kesv has a high ($P = 0.8$) and Kcv only a low ($P = 0.4$) probability of being targeted to the mitochondria (Table S1). Indeed, a chimera (NT-Kesv:GFP) comprising the Kesv N terminus (M^1-T^{36}) plus GFP was found to accumulate in the mitochondria of HEK293 cells; this apparent accumulation in the mitochondria, which occurs on a large background of GFP signal in the cytoplasm, did not occur when the 2 critical arginines (R^3, R^4) in NT-Kesv:GFP were mutated to glutamines (Fig. S4 *A* and *B*). Collectively, these experiments support the prediction that the Kesv N-terminal domain could promote mitochondria import; the weak mitochondrial accumulation over a large cytoplasmic background nonetheless implies that this signal is not very strong.

To further test the signal peptide nature of the Kesv N terminus, we prepared 3 plasmid constructs to examine its significance in targeting the entire Kesv:GFP protein to the mitochondria: (*i*) mutations were produced in key amino acids in the putative Kesv signal peptide domain, (*ii*) the signal peptide was fused to Kcv, and (*iii*) the Kesv N terminus was replaced by that of Kcv.

The results with all 3 constructs in transfected HEK293 cells (Fig. 4 *B* and *C* and Fig. S4*C*; see above) established that the Kesv N-terminal signal peptide is neither required for mitochondrial targeting nor strong enough to impose mitochondrial targeting. Fig. 4*A* shows an example of the distribution of Kesv:GFP containing the critical mutations (R^3E, R^4E) in the signal peptide. Despite the low predicted probability (Table S1), the construct still accumulates in the mitochondria (Fig. 4 *A* and *C*).

CELL BIOLOGY

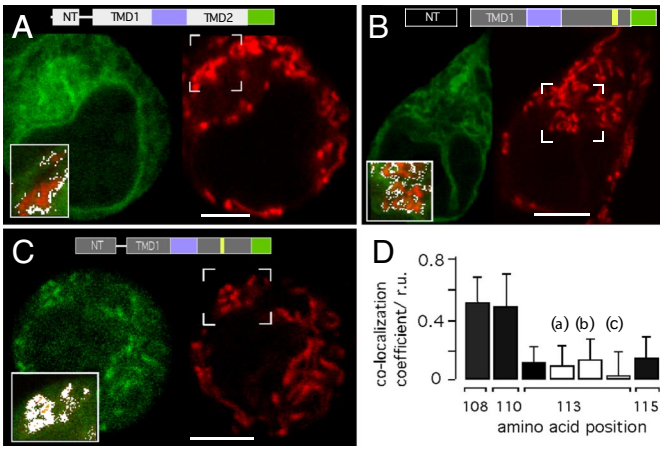

Fig. 5. The second TMD determines targeting of viral K^+ channels. (*A–C*) (*Top*) color-coded structural elements of chimeras (see Fig. 2). The location of the insertion of the 3-amino acids IVL is indicated in yellow. (*A–C*) Images of GFP (green) and MitoTracker (red) channels from confocal images of exemplary HEK293 cells expressing different chimeras of Kesv:GFP or Kcv:GFP. *Insets* show overlay of the green and red channels from areas indicated. White pixels highlight areas of maximal colocalization. (*A*) Chimera of Kcv:GFP in which the pore of this channel has been replaced with the pore of channel Kesv. Chimera of Kesv:GFP in which TM2 has been extended at position 113 (*B*) or at position 108 (*C*) by the 3-aa IVL. (*D*) Pearson's colocalization coefficient (*P*) for GFP and MitoTracker red in HEK293 cells expressing Kesv:GFP constructs in which TM2 was extended in the positions indicated. P was determined as shown in Fig. 2. The filled bars illustrate extensions by amino acids motive VVV. For the remaining extensions the amino acids motives VV (bar a), IVL (bar b), and IVLIVL (bar c) were used. Mean values ± standard deviation from ≥10 images.

The same result was obtained after mutating the 2 remaining positively charged amino acids (R^{16} or K^{25}) in the signal peptide, which might be involved in mitochondrial sorting (Table S1). Finally, when the entire N terminus of Kesv (M^1-T^{36}) was replaced with the Kcv N terminus (M^1-E^{12}), the protein still accumulated in the mitochondria (Fig. 4*C*).

These results established that the Kesv N-terminal signal peptide was able to direct GFP to the mitochondria (Fig. S4 *A* and *B*). However, when the signal peptide was fused to Kcv, the protein sorted to the secretory pathway; thus the signal peptide failed to impose sorting to the mitochondria. This fusion protein still enters the secretory pathway (Fig. 4 *B* and *C*).

Collectively, these experiments establish that the N terminus of Kesv is neither sufficient nor essential to determine the sorting of the channel proteins; other signals must be present in the 2 channels, which determine their destination.

A Sorting Signal Is Associated with the Inner Transmembrane Domain. To identify other relevant sorting signals, we constructed a chimera protein [Kcv(P)Kesv:GFP] in which the pore of Kcv (E^{30}-K^{72}) was replaced with the Kesv pore (D^{60}-L^{92}). This chimera protein should reveal whether the sorting information is associated with the pore or with the transmembrane domains. The results show that this chimera is no longer targeted to the mitochondria but enters the secretory pathway when it is expressed in HEK293 cells (Fig. 5*A*). This result implies that at least some sorting information is contained in the TMDs.

Interestingly, program TMHMM2.0, an algorithm that predicts the length of TMDs (16), indicates that the first and second TMD of eukaryotic and prokaryotic K^+ channel proteins with 2 TMDs are 23 aa long. However, the second TMD in the 2 viral channels is significantly shorter than those of all other K^+ channels with the same predicted architecture. In particular, the length of Kesv TM2 is predicted to be 2 aa shorter than Kcv TM2 (Table S2). Also, TM2 of Kesv is predicted to start further downstream than that of Kcv (Fig. S1*A*). These predicted differences in TM length and in position occur despite the high amino acids identity in this region for the 2 proteins.

To examine the relevance of the TMD length to channel localization and function, we extended the C-terminal portion of the Kesv TMD2 by adding 2–6 hydrophobic amino acids in position 113 of Kesv:GFP. The different constructs and their predicted effects on TM2 length and on the energy for partitioning into the membrane (17) are presented in (Table S2).

Fig. 5*B* shows an example of the cellular distribution of a Kesv:GFP protein in which TM2 was extended by 3 hydrophobic amino acids (IVL) in position 113. The protein no longer colocalizes with MitoTracker red but mimics the distribution of Kcv:GFP (Fig. 5 *B* and *D*). This is apparent from the perinuclear distribution of GFP and the apparent separation of GFP and MitoTracker red fluorescence, as well as the low colocalization coefficient (Fig. 5*D*). This same qualitative result was obtained if the extension consisted of the amino acid motif VVV rather than IVL (Fig. 5*D*). Similar localization results were obtained if 2, 3, or 6 hydrophobic amino acids were inserted in this position (Fig. 5*D*). However, visual inspection of the images, as well as colocalization analyses, indicate that sorting of the Kesv:GFP mutant to the secretory pathway is strongest when 6 aa are added to TM2.

After determining that the length of TM2 was important for sorting, we examined whether length was solely responsible for sorting. Therefore, the Kesv:GFP protein was extended by the 3-amino acids IVL at amino acids positions 108, 110, and 115. The resulting cellular distribution of these constructs was compared with that obtained with the extension in position 113. Inspection of the image (e.g., Fig. 5*C*), as well as colocalization analyses (Fig. 5*D*), reveals that the TM2 extension is position dependent and not determined by the physicochemical properties of the TMDs (Table S2). Only extension of TM2 in the downstream end (≥ position 113) shifted sorting from the mitochondria to the secretory pathway. The 2 upstream extensions had no impact on sorting; a representative image of a HEK293 cell expressing Kesv:GFP with a 3-amino acids extension in position 108 indicates that this construct primarily colocalizes with the mitochondria (Fig. 5 *C* and *D*).

Kesv with Modified Targeting Signals Generates K^+ Conductance. The results suggest that redirection of a channel protein from sorting to the mitochondria to the secretory pathway leads to active channels in the plasma membrane. These results also predict that only those constructs that reach the secretory pathway should rescue the Δ*trk1*, Δ*trk2* yeast mutant in low K^+. The results presented in Fig. 1 substantiate this prediction. Transformation of yeast mutants with either $Kesv^{113}VV$, $Kesv^{113}VVV$, or Kcv(NT)Kesv [i.e., those proteins that are sorted into the secretory pathway in HEK293 cells (Figs. 4 and 5)] support yeast growth on low-K^+ concentrations. Channel mutants that maintained their mitochondrial sorting did not rescue the yeast mutants on low-K^+ medium (Fig. 1). Worth noting is that this general conclusion is supported by the imaging data using GFP-tagged proteins as well as by the yeast rescue assay and the mitochondria import study (Fig. 3), which both rely on untagged proteins. This means that the tag has no major impact on the general distribution of the proteins.

To further examine the ability of Kesv to function as a K^+ channel we also tested 2 chimeras in HEK293 cells for conductance: (*i*) the chimera Kcv(P)Kesv:GFP, in which the Kcv pore domain was replaced with the Kesv pore domain (Fig. 5*A*), and (*ii*) 2 mutants of Kesv in which TM2 was extended at position 113 by either 3 or 6 aa (Fig. 5*B*).

Data in Fig. S5 *A* and *B* show the typical current responses of HEK293 cells transfected either with GFP or with Kcv(P)Kesv:GFP in a standard clamp protocol. The current families and the

I/V relations indicate that Kcv(P)Kesv:GFP-transfected cells produced currents different from WT cells but with features similar to those in Kcv:GFP-transfected cells (10). The I/V relation had the typical Kcv features with a characteristic decrease in current at negative clamp voltages. The inward current in cells expressing this conductance was at a reference voltage of −100 mV, approximately 10 times higher than in non- or mock-GFP-transfected cells. Furthermore, the conductance of the Kcv(P)Kesv:GFP-transfected cells had a greater dependence on external K^+ concentration than the controls (Fig. S5*E*). On average, the reversal voltage shifted in the former cells for a 10-fold increase in K^+ by 48 ± 2 mV ($n = 8$). The same increase in K^+ only resulted in a shift of 13 ± 4 mV ($n = 20$) in control cells. This result implies that the increased conductance is due to a functional K^+ channel. Hence the chimera containing the Kesv pore produces a conductance with features of a K^+ channel.

Similar currents were recorded, albeit at a lower frequency, when Kesv:GFP containing a TM2 extended in position 113 by either 3 or 6 aa (+IVL or +IVLIVL) was expressed in HEK293 cells (Fig. S5 *C–E*). The K^+ conductance was significantly elevated over that of control cells. It should be noted that the I/V relations of the 2 constructs ($Kesv^{113}$IVL:GFP and Kcv(P)Kesv:GFP) are similar to one another. In both channels, the I/V relation has a characteristic saturation at very negative voltages.

Discussion

Viruses PBCV-1 and EsV-1 are both members of the family *Phycodnaviridae* and clearly have a common evolutionary ancestor. However, they have different hosts, habitats, and life cycles, suggesting that a long time has elapsed since they diverged (11). Despite these differences, they both code for proteins that form K^+ channels. One protein, Kcv, has previously been shown to form a functional K^+ channel (8). The present results show that a second virus-encoded channel, Kesv, has the functional properties of a canonical K^+ channel in the plasma membrane of mammalian cells. However, channel activity only occurs after the protein is targeted to the plasma membrane. In contrast to a previous report (12), we found no Kesv-mediated plasma membrane conductance.

The discovery of 2 functional K^+ channels in different viruses is interesting from a virology viewpoint. Both viruses have large genomes, >330 kb, and encode 231 (EsV-1) or 366 (PBCV-1) proteins. However, they only encode 33 proteins in common, including the two K^+ channels (11). Intuitively, one would predict that common conserved genes between the 2 viruses would encode proteins with a similar function(s) in the life cycles of the 2 viruses. The present experiments do not directly address the question of the function of the 2 K^+ channels, but the fact that the 2 proteins have different targeting properties in heterologous systems suggests that they also have different functions in their hosts. The Kesv protein probably performs in the mitochondria of its host. Because of the central function of mitochondria in cells, these organelles seem to be a preferred target of viral channels. For example, the PB1-F2 protein from influenza A virus and the channel-forming p7 protein from hepatitis C virus are targeted to this organelle (18, 19).

The most interesting finding in the present study is that both channel proteins are similar in terms of their predicted primary structure. However, in heterologous systems one channel is targeted to the plasma membrane through the secretory pathway and the other one into the mitochondria. The exact mode for the import is not yet known, but the data indicate that it occurs like that of many other hydrophobic mitochondrial proteins in a voltage-dependent manner through the canonical TOM complex. Once imported into the mitochondria the channel seems to assemble as a tetramer.

The sorting of viral channels in heterologous systems is artificial. Nonetheless, the differential sorting of the 2 viral channels occurs both in mammalian cells and in yeast. Hence, the results are not just a property of a specific cell type; the results reveal the mechanistic ability of cells to sort similar membrane proteins between mitochondria and the secretory pathway.

Import of proteins into mitochondria occurs through 1 of 2 pathways, each involving a distinct import machinery and sorting signals (20). One pathway relies on a cleavable N-terminal targeting sequence, the other pathway, which is more characteristic of hydrophobic proteins, uses internal targeting sequences. The present data indicate that neither of these mechanisms is exclusively responsible for sorting the viral K^+ channels. Targeting of these virus channels must be understood in the context of a concerted function of more than 1 sorting signal. Our results are consistent with the following model: the mitochondria-targeted Kesv channel has an N-terminal domain that resembles a cleavable mitochondrial signal peptide; like typical mitochondrial signal peptides it consists of an α-helix with positively charged amino acids (15). Its function as a mitochondrial-targeting domain is supported by the fact that it can direct a GFP protein to HEK293 mitochondria. Nonetheless, this import signal must be weak in heterologous expression systems. In the context of the complete Kesv protein, this domain is neither required for mitochondrial targeting nor does it confer mitochondrial sorting when fused to Kcv. This finding is surprising because other membrane proteins targeted to the mitochondria require this N-terminal domain (21). The import of a chimera containing the Kcv channel, with the Kesv N-terminal signal sequence, into the secretory pathway establishes that such a mitochondrial import signal is in context of the Kcv protein weaker than an intrinsic ER signal of the latter channel.

A strong sorting signal is associated with the fold in the downstream portion of TM2. The importance of this domain is revealed by the finding that certain site-specific ≥2-aa extensions to Kesv TM2 are sufficient to shift the destination of the protein from the mitochondria to the secretory pathway. These results convincingly demonstrate that the site-specific length of TM2, rather than an internal targeting signal (18, 22), is responsible for sorting the channels between different destinations.

The present results are relevant in the context of a yet-unresolved question about targeting membrane proteins in eukaryotes. It is not understood how the same or very similar proteins (4) or isoforms of membrane proteins, such as Kv channels or the ATP-regulated K^+ channel protein, are sorted to the mitochondria, whereas nearly identical proteins travel to the plasma membrane (3). The present experiments provide some information on this process because the results suggest that the recognition sites for the import machineries into mitochondria and the ER have a high degree of tolerance. They can successfully compete for the same K^+ channel proteins. Apparently, only minor structural differences in the TMD of a protein are sufficient to direct it to a sorting pathway. In this context, the sorting of K^+ channel proteins can be understood in the same way as that of several other proteins for which a combination of sequence elements provides flexibility for protein targeting to diverse compartments (6).

The fact that the decision for sorting relies on a structure near the C terminus of the 2 viral channel proteins is surprising. This result means that the sorting does not occur during the synthesis of these proteins because typically, direct translocation into the mitochondria or the ER proceeds in a cotranslational manner beginning with the N terminus of the protein. The C-terminal localization of the signal domain in the 2 viral proteins means that structural features, which affect protein folding/unfolding are probably essential for targeting the small viral K^+ channel proteins (18, 23).

The overall similarity in the architecture of the viral channels to eukaryotic K^+ channels implies that similar mechanisms may

also be relevant in the sorting of these eukaryotic channel proteins to different organelles.

Materials and Methods

Constructs and Mutagenesis. For expression in HEK293 cells, Kcv or Kesv genes were cloned into the BglII and EcoRI sites of the pEGFP-N2 vector (Clontech) in frame with the downstream EGFP gene by deleting the Kcv and Kesv stop codon. Point mutations were created by the QuikChange method (Stratagene) and confirmed by DNA sequencing. Chimeras of Kesv and Kcv were created by sequential PCRs according to strategies described in ref. 24. The chimeras comprised the following elements: (*i*) Kesv(NT)Kcv: the Kesv N terminus (NT) was replaced with the Kcv N terminus [Kcv (M^1-E^{12}) and Kesv (S^{37}-K^{124})]; (*ii*) Kcv(NT)Kesv: the Kcv NT was replaced with the Kesv N terminus [Kesv (M^1-T^{36}) plus Kcv (P^{13}-L^{94})]; (*iii*) Kcv(TM2)Kesv: the Kcv TM2 was replaced with the Kesv TM2 [Kcv (M^1-D^{68}) plus Kesv (L^{92}-K^{124})]; (*iv*) Kesv(TM2)Kcv: the Kesv TM2 was replaced with the Kcv TM2 [Kesv (M^1-D^{91}) plus Kcv (I^{69}-L^{94})]; (*v*) Kcv(P)Kesv: the Kcv P was replaced with Kesv P [Kcv (M^1-F^{35}) plus Kesv (D^{60}-L^{92}) plus Kcv (T^{74}-L^{94})].

For expression in yeast, K^+ channels and mutants were cloned into a derivative of pYES2 vector (Invitrogen) as described in ref. 25.

Expression of Channel Proteins and Electrophysiology. Cell culture, transfection protocols and methods for recording membrane currents in HEK293 cells were performed as described elsewhere (10).

Confocal Microscopy. HEK293 cells were investigated approximately 24 h after transfection with a Leica TCS SP spectral confocal microscope equipped with an argon/krypton laser (Leica Microsystems). Images were acquired with an HCX PL APO 63×/1.2w objective. EGFP was excited with a 488-nm argon laser line, and confocal sections were collected using a 505–530-nm emission setting. MitoTracker red CMXRos (Invitrogen) was excited with a 543-nm helium neon laser line and emission collected at 600–630 nm. For mitochondrial staining, cells were incubated with 300 nM MitoTracker for 30 min before imaging. Images and colocalization were analyzed with ImageJ software (National Institutes of Health).

***Saccharomyces cerevisiae* Complementation Assays.** Selection experiments were performed as reported (25). Viral K^+ channels or their mutants were transformed into SGY1528 yeast strain (*Mat a ade*2–1 *can*1–100 *his*3–11,15 *leu*2–3,112 *trp*1–1 *ura*3–1 *trk*1::HIS3 *trk*2::TRP1), which are deficient in endogenous K^+ uptake systems. Yeasts from the same stock were grown in parallel under nonselective conditions on plates containing 100 mM KCl and on selective conditions on agar containing 1 mM KCl or 0.5 mM KCl. Growth experiments were performed at 30°C.

Mitochondrial Import of Kesv. Transcription and translation as well as [^{35}S] methionine labeling were performed in a rabbit reticulocyte lysate Kit (T7 TNT Quick coupled transcription/translation; Promega) as described previously (26). Mitochondrial import of radiolabeled proteins into isolated mitochondria from *S. cerevisiae* (WT YPH499) was examined according to standard procedures described earlier (26). Isolated mitochondria were generally resuspended in buffer containing 250 mM sucrose, 1 mM EDTA, and 10 mM Mops-KOH (pH 7.2), without or with 600 mM NaCl.

Where indicated (-$\Delta\psi$), 1 μM valinomycin was added to isolated mitochondria to discharge the membrane potential. All import assays were carried out at 25°C. For protease treatment, the samples were cooled to 0°C and incubated with 200 μg/ml of proteinase K for 20 min at 0°C. The samples were subsequently incubated with 1.5 mM PMSF for 5 min at 0°C. The mitochondria were re-isolated by centrifugation (10 min 16 000 $\times$ *g*) and analyzed by SDS/PAGE and fluorography. Blue native polyacrylamide gel electrophoresis was carried out by analyzing yeast mitochondria, solubilized in the presence of 1% (wt/vol) digitonin, in native conditions as described earlier (26).

ACKNOWLEDGMENTS. We thank Adam Bertl (Darmstadt) for advice with yeast rescue experiments; Massimo Zeviani (Milano) for discussions on mitochondrial proteins; and Marina Alber for help in the import studies. The *tom22*Δ yeast mutant and the Tom40 antiserum were kindly provided by Nikolaus Pfanner (Freiburg). This work was supported in part by Deutsche Forschungsgemeinschaft (GRK340) (to G.T.), SPP1131 (to J.R.), Public Health Service Grant GM32441 (to J.V.E.), and National Institutes of Health (NIH) grant P21RR15635 from the COBRE program of the National Center for Research Resources (to J.V.E.). D.L.M. was supported by grants from the McKnight Foundation for Neuroscience and the NIH; and A.M. by Ministero dell'Università e della Ricerca Scientifica, Progetto Prin 2005.

1. Pelkmans L, Helenius A (2003) Insider information: what viruses tell us about endocytosis. *Curr Opin Cell Biol* 15:414–422.
2. Sollner TH (2004) Intracellular and viral membrane fusion: a uniting mechanism. *Curr Opin Cell Biol* 16:429–435.
3. Miyazaki E, Kida Y, Mihara K, Sakaguchi M (2005) Switching the sorting mode of membrane proteins from cotranslational endoplasmic reticulum targeting to post-translational mitochondrial import. *Mol Biol Cell* 16:1788–1799.
4. Karniely S, Pines O (2005) Single translation-dual destination: mechanism of dual protein targeting in eukaryotes. *EMBO J* 6:420–425.
5. White SH, von Heijne G (2008) How translocons select transmembrane helices. *Annu Rev Biophys* 37:23–42.
6. Hegde RS, Bernstein HD (2006) The surprising complexity of signal sequences. *Trends Biochem Sci* 31:563–571.
7. Szabò I, *et al.* (2005) A novel potassium channel in lymphocyte mitochondria. *J Biol Chem* 280:12790–12798.
8. Plugge B, *et al.* (2000) A potassium ion channel protein encoded by chlorella virus PBCV-1. *Science* 287:1641–1644.
9. Pagliuca C, *et al.* (2007) Molecular properties of Kcv a viral-encoded K^+ channel. *Biochem* 46:1079–1090.
10. Hertel B, *et al.* (2006) Elongation of outer transmembrane domain alters function of miniature K^+ channel Kcv. *J Membr Biol* 210:21–29.
11. Van Etten JL, Graves MV, Müller DG, Boland W, Delaroque N (2002) Phycodnaviridae-large DNA algal viruses. *Arch Virol* 147:1479–1516.
12. Chen J, Cassar SC, Zhang D, Gopalakrishnan M (2005) A novel potassium channel encoded by *Ectocarpus siliculosus* virus. *Biochem Biophys Res Commun* 326:887–893.
13. Minor DL, Masseling SJ, Jan YN, Jan LY (1999) Transmembrane structure of an inwardly rectifying potassium channel. *Cell* 96:879–891.
14. van Wilpe S, *et al.* (1999) Tom22 is a multifunctional organizer of the mitochondrial preprotein translocase. *Nature* 401:485–489.
15. Schwarz E, Neupert W (1994) Mitochondrial protein import: Mechanisms, components and energetics. *Biochim Biophys Acta* 1187:270–274.
16. Möller S, Croning MDR, Apweiler R (2001) Evaluation of methods for the prediction of membrane spanning regions. *Bioinformatics* 17:646:653.
17. White SH, Wimley WC (1999) Membrane protein folding and stability: physical principles. *Annu Rev Biophys Biomol Struct* 28:319–365.
18. Gibbs JS, Malide D, Hornung F, Bennink JR, Yewdell JW (2003) The influenza A virus PB1–F2 protein targets the inner mitochondrial membrane via a predicted basic amphipathic helix that disrupts mitochondrial function. *J Virol* 77:7214–7224.
19. Griffin SD, Harvey R, Clarke DS, Barclay WS, Harris M, *et al.* (2004) A conserved basic loop in hepatitis C virus p7 protein is required for amantadine-sensitive ion channel activity in mammalian cells but is dispensable for location to mitochondria. *J Gen Virol* 85:451–461.
20. Chacinska A, Pfanner N, Meisinger C (2002) How mitochondria import hydrophilic and hydrophobic proteins. *Trends Cell Biol* 12:299–302.
21. Graf SA, Haigh SE, Corson ED, Shirihai OS (2004) Targeting, import and dimerization of a mammalian mitochondrial ATP binding cassette (ABC) transporter, ABCB10 (ABC-me). *J Biol Chem* 279:42954–42963.
22. Endo T, Kohda D (2002) Functions of outer membrane receptors in mitochondrial protein import. *Biochim Biophys Acta* 1592:3–14.
23. Wilcox A, Choy J, Bustamante C, Matouschek A (2005) Effect of protein structure on mitochondrial import. *Proc Natl Acad Sci USA* 102:15435–15440.
24. Pytela R, Suzuki S, Breuss J, Erle DJ, Sheppard D (1994) Polymerase chain reaction cloning with degenerate primers: homology-based identification of adhesion molecules. *Methods Enzymol* 245:420–451.
25. Minor DL, Masseling SJ, Jan YN, Jan LY (1999) Transmembrane structure of an inwardly rectifying potassium channel. *Cell* 96:879–891.
26. Papatheodorou P, Domanska G, Rassow J (2007) Protein targeting to mitochondria of *Saccharomyces cerevisiae* and *Neurospora crassa*. *Methods Mol Biol* 390:151–166.

Supporting Information

Balss *et al.* 10.1073/pnas.0805709105

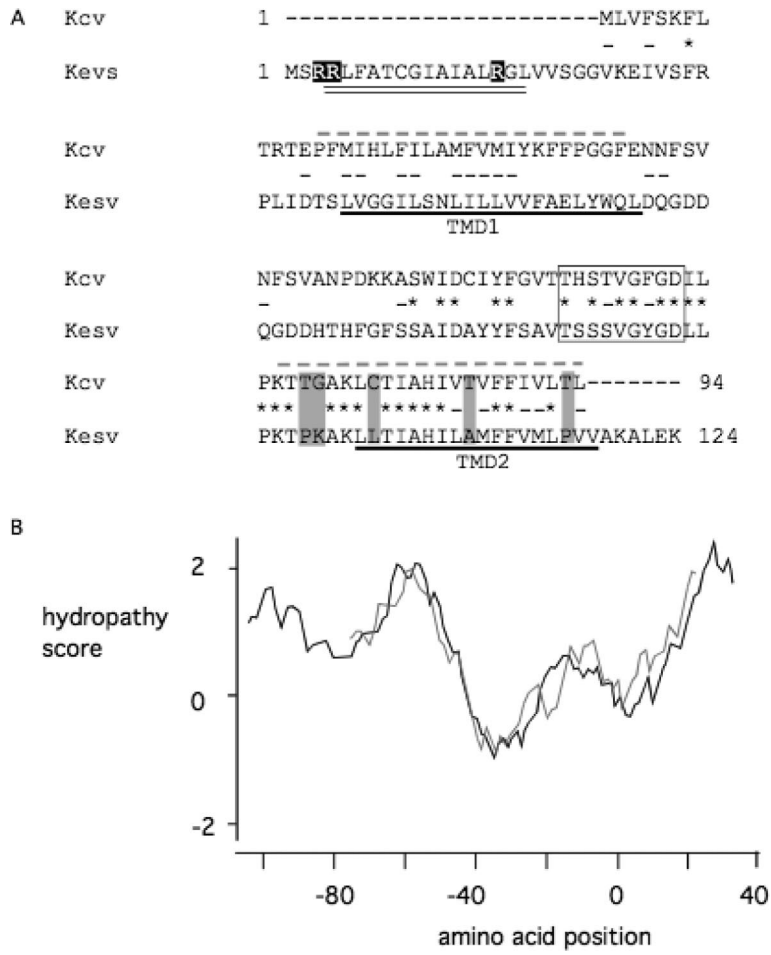

Fig. S1. K^+ channel homologues coded by 2 algal viruses. (*A*) Alignment of predicted amino acid sequences of K^+ channel proteins Kcv from chlorella virus PBCV-1 and Kesv from virus EsV-1. Both sequences have an overall 55% similarity (−) and 29% amino acid identity (asterisk). The position of the predicted selectivity filter is boxed. The positions of TM domains predicted by TMHMM-2.0 algorithm are shown by bars (Kesv) and dashed lines (Kcv). Four different structure prediction programs (see Materials and Methods) indicate the presence of an α-helix (double line) in the N terminus of Kesv. The positive amino acids highlighted in the N terminus of Kesv are critical for the signal peptide nature of this domain. (*B*) Hydrophobicity profile of the 2 proteins (Kesv, black line; Kcv, gray line) calculated according to the Kyle and Doolittle algorithm with a moving window of 15 aa and plotted against amino acid number. The two sequences were normalized (amino acid position 0) to the common selectivity filter motive GYG/GFG.

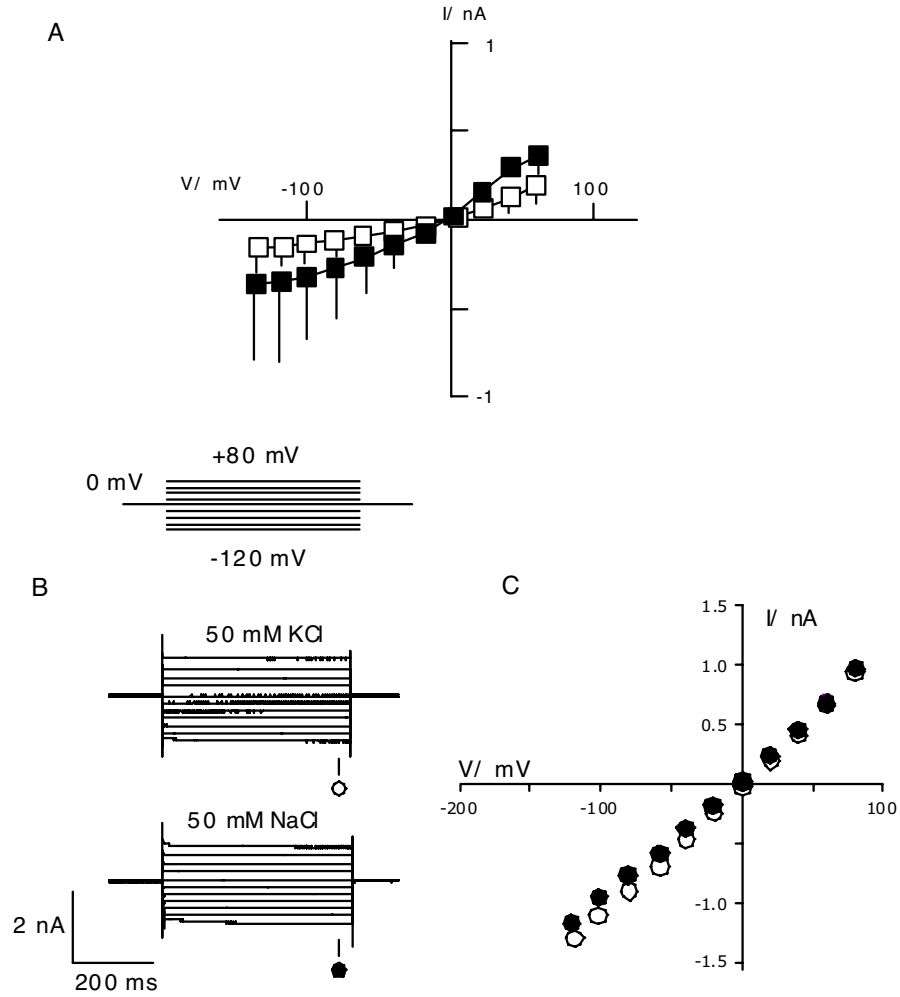

Fig. S2. Expression of Kesv:GFP generates no appreciable K^+ conductance in HEK293 cells. (*A*) Steady-state I/V relation of HEK293 cells expressing only GFP (open square, $n = 20$) or Kesv:GFP (filled square, $n = 23$). The Kesv:GFP-expressing cells exhibit no significant increase in conductance. Only the SD is higher compared with the control. Occasionally we observed some cells with more current than control cells; one example is shown in (*B*). In these cases, however, the currents were insensitive to changes in the K^+ concentration in the bath medium (data not shown) or to a replacement of K^+ by Na^+ (*B*). The steady-state I/V relation of the data in *B* reveals no appreciable difference between the currents recorded in K^+ (open circles) or Na^+ (filled circles) (*C*).

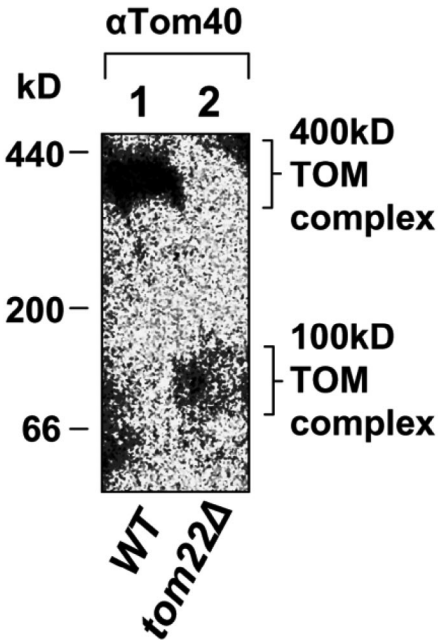

Fig. S3. Tom 22D mutant has a corrupted Tom complex. WT and *tom22*Δ mitochondria, respectively, were lysed in the presence of digitonin and analyzed by blue native PAGE as described in Materials and Methods. The proteins were blotted on a PVDF membrane, and Tom40 was visualized using a polyclonal antiserum.

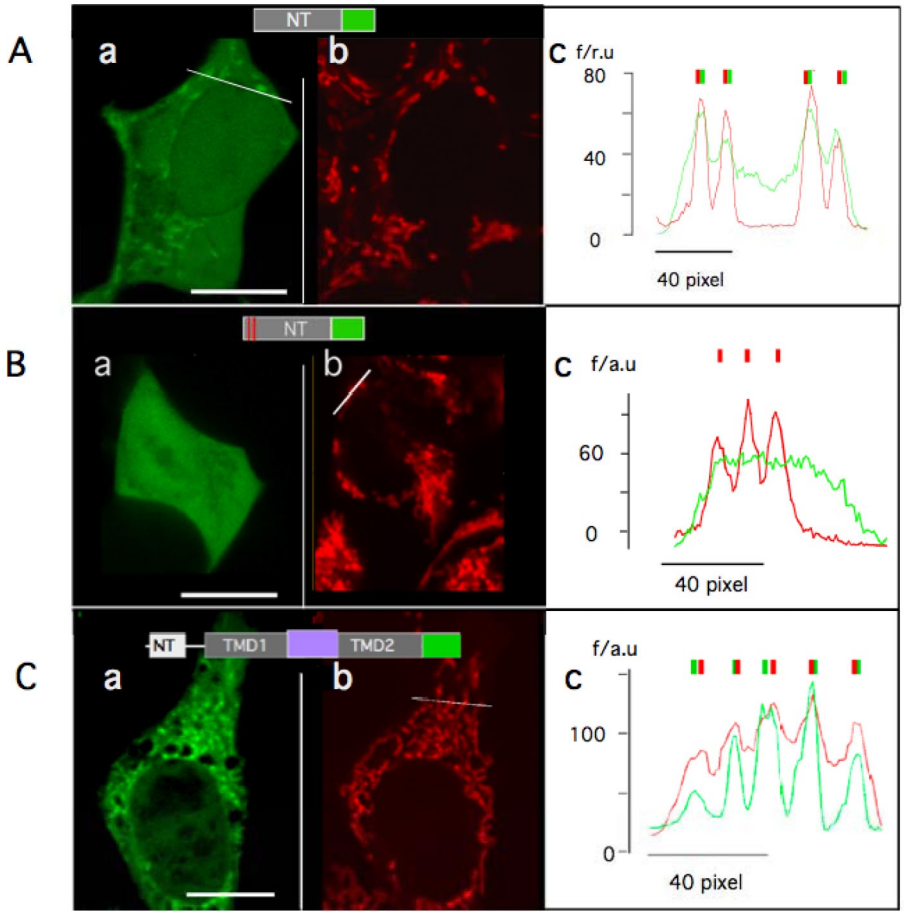

Fig. S4. The N-terminus of a channel does not determine localization. (*A*) Confocal images of exemplary HEK293 cell expressing chimera comprising N-terminal domain (NT) of Kesv (MI-T36) plus GFP. The green channel shows the distribution of GFP (*a*) the red channel the fluorescence of mitotracker red (*b*). Intensity plot (*c*) from line scan of GFP (green) and mitotracker (red) fluorescence in region of the white line in *b*. Note coincidence of fluorescent maxima. (*B*) Same as in *A* but with mutation (R3E, R4E) of charges in N-terminal domain. Note the absence of distribution maxima of GFP in *a* and *c*. (*C*) Confocal image of exemplary HEK293 cell expressing chimera of Kesv:GFP in which the N-terminus was replaced by that of Kcv (*a*) and staining of the same cell with mitotracker red (*b*). Intensity plot (*c*) from line scan of GFP (green) and mitotracker (red) fluorescence in region of the white line in *a*. Note the alternating position of red and green intensity peaks. Scale bars: 10 μm.

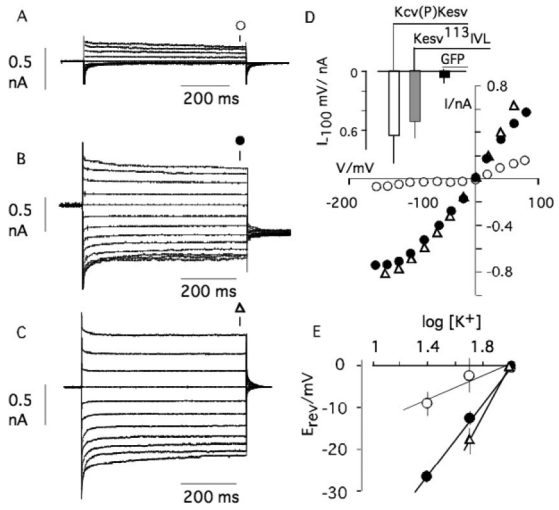

Fig. S5. Kesv mutants with altered sorting signals generate conductance with moderate K^+ selectivity in plasma membrane of HEK293 cells. Representative current responses to standard clamp protocol (holding voltage: 200 ms, 0 mV; test voltages: 600 ms + 80 mV to ≥ −120 mV; post voltage: ≥100 ms, 0 mV) in a HEK293 cell transfected with only GFP (*A*), with Kcv(P)Kev:GFP (*B*), or a mutant of Kesv:GFP with an extension of TM2 by 3 aa (Kesv^{113}IVL:GFP) (*C*). The symbols in *A*–*C* indicate the point of data collection and cross-reference with symbols in (*D*), which shows the corresponding steady-state current/voltage (I/V) relations. Inset in *D* shows the mean steady-state currents (± SD) at −100-mV test voltage from cells transfected with Kcv(P)Kev:GFP (open bar, $n = 19$) or Kesv^{113}IVL:GFP (gray bar, $n = 6$) compared with mock GFP-transfected or untransfected HEK293 cells (solid bar, $n = 25$). (*E*) Nernst plots of mean reversal voltages (± SD, $n \geq 3$) obtained from instantaneous I/V relations in bath solutions with different K^+ concentrations from HEK293 cells transfected with Kcv(P)Kev:GFP (filled circle), Kesv:GFP^{113}IVL (open triangle), or mock-transfected cells (open circle).

Table S1. Prediction for targeting and experimental localization of Kcv:GFP, Kesv:GFP, and its mutants

Channel	Prediction		Experimental localization
	Mitoprot	TargetP	
Kcv	0.4	0.02	sp
Kesv	0.8	0.63	mi
KesvR^{3}ER^{4}E	0.2	0.09	mi
KesvR^{16}E	0.7	0.14	mi
KesvR^{16}S	0.5	0.30	mi
KesvK^{25}E	0.8	0.40	mi
KesvR^{3}ER^{4}ER^{16}E	0.1	0.04	mi
KesvR^{3}ER^{4}ER^{16}S	0.1	0.04	mi
GFP	0.06	0.03	ud
Kesv(NT):GFP	0.8	0.50	mi
Kesv(NT)R^{3}ER^{4}E:GFP	0.2	0.06	ud
Kcv(NT)Kesv:GFP	0.8	0.60	sp
Kesv(NT)Kcv:GFP	0.5	0.02	mi

The predictions were calculated using Mitoprot (1) and TargetP (2) prediction algorithms. The localization of the proteins either in mitochondria (mi) or the secretory pathway (sp) or in an undefined location (ud) was determined from confocal images.

1. Claros MG, Vincens P (1996) *Eur J Biochem* 241:779–786.
2. Emanuelsson O, Nielsen H, Brunak S, von Heijne G (2000) *J Mol Biol* 300:1005–1016.

Table S2. Physicochemical properties and cellular localization of viral channels Kcv and Kesv

	oct (ΔG(kcal/mol))	int	TM	Destination
Kcv	7.3	3.0	20 (20)	sp
Kesv	11.4	4.1	18 (23)	mi
Kesv^{113}VV	12.3	4.2	23	sp
Kesv^{113}VVV	12.3	4.2	23	sp
Kesv^{108}IVL	13.8	5.2	23	mi
Kesv^{110}IVL	13.8	5.2	23	mi
Kesv^{113}IVL	13.8	5.2	23	sp
Kesv^{115}IVL	13.8	5.2	23	sp
Kesv^{113}IVLIVL	14.9	5.7	23	sp

The data reveal the calculated Gibbs free energy [ΔG (kcal/mol)] for partitioning of TM2 from Kcv, Kesv, and mutants from bilayer into water. Data obtained by using the Membrane Explorer Program and the Wimley and White scale (1) for a 19-aa-long transmembrane domain with amino acids 110 for Kesv and 86 for Kcv in the center. The data provide values for transition energy from the octonal face (oct) and for the interface (int) to water. Also shown is the predicted number of amino acids in TM2 of the respective channels as calculated by the TMMHMM2.0 algorithm. The data calculated, including the GFP and linker, are given in parentheses. sp, secretory pathway; mi, mitochondria.

1. White SH, Wimley WC (1999) *Annu Rev Biophys Biomol Struc* 28:319–365.